

IUCrJ

Volume 4 (2017)

Supporting information for article:

A closer look at close packing: pentacoordinated silicon in a high-pressure polymorph of danburite

A. Pakhomova, E. Bykova, M. Bykov, K. Glazyrin, B. Gasharova, H.-P. Liermann, M. Mezouar, L. Gorelova, S. Krivovichev and L. Dubrovinsky

Table S1. Crystallographic data and refinement parameters for danburite polymorphs

Crystal data	1.1(1) GPa	22.6(1) GPa	25.4(1) GPa	25.4(1) Pa	32.3(1) GPa
	Danburite		Danburite-II	Danburite-III	Danburite-IV
Space group	<i>Pnam</i>	<i>Pnam</i>	<i>Pnam</i>	<i>P-1</i>	<i>P2₁/c</i>
<i>a</i> , Å	8.0035(2)	6.8576(3)	6.3537(5)	5.479(5)	7.9989(17)
<i>b</i> , Å	8.7386(3)	8.1526(3)	7.9518(3)	5.532(2)	7.8697(14)
<i>c</i> , Å	7.7147(2)	7.7457(2)	8.0112(3)	6.681(6)	6.249(3)
α , °	90	90	90	91.74(5)	90
β , °	90	90	90	104.57(8)	89.75(3)
γ , °	90	90	90	95.59(5)	90
Volume, Å ³	539.56(3)	433.04(3)	404.75(4)	194.7(3)	393.4(2)
<i>Z</i>	4	4	4	2	4
Data collection					
Wavelength, Å	0.29024	0.29024	0.29056	0.29056	0.29056
Max. θ °	17.189	16.875	16.730	11.151	10.458
Index ranges	-14≤ <i>h</i> ≤13 -13≤ <i>k</i> ≤12 -13≤ <i>l</i> ≤14	-10≤ <i>h</i> ≤11 -13≤ <i>k</i> ≤12 -13≤ <i>l</i> ≤15	-10≤ <i>h</i> ≤9 -13≤ <i>k</i> ≤12 -15≤ <i>l</i> ≤14	-6≤ <i>h</i> ≤6 -7≤ <i>k</i> ≤7 -8≤ <i>l</i> ≤7	-9≤ <i>h</i> ≤9 -9≤ <i>k</i> ≤9 -6≤ <i>l</i> ≤6
No.meas.refl.	3169	2397	2163	1042	940
No.uniq.refl.	1322	977	891	591	524
No. obs.refl	1241	926	742	397	408

$(I > 2\sigma(I))$ *Refinement of the structure*

No.of variables	64	65	65	68	68
R_{int}	0.0251	0.0191	0.0239	0.0545	0.0536
R_{σ}	0.0303	0.0229	0.0291	0.0934	0.0587
$R_1, I > 2\sigma(I)$	0.0219	0.0262	0.0423	0.1154	0.0982
R_1 , all data	0.0235	0.0293	0.0596	0.0887	0.1254
w $R_2, I > 2\sigma(I)$	0.0651	0.0698	0.1256	0.2368	0.2944
w R_2 , all data	0.0663	0.0723	0.1783	0.2714	0.3099
GooF	1.218	1.190	1.321	1.120	1.178

Table S2. Bond distances and polyhedral parameters in danburite, $\text{CaB}_2(\text{SiO}_4)_2$

Pressure	1.1(1) GPa	22.6(1) GPa	25.4(1) GPa	32.3(1) GPa				25.4(1) GPa			
Phase	Danburite		Danburite-II	Danburite-IV			Danburite-III				
CN(Si)	<i>Pnam</i>		<i>Pnam</i>	<i>P2_1/c</i>			<i>P-1</i>				
<i>SiO_n</i> polyhedra											
	<i>SiO₄</i>		<i>SiO₅</i>	<i>SiIO₅</i>		<i>Si2O₅</i>	<i>SiIO₆</i>		<i>Si2O₆</i>		
Si-O3	1.6119(7)	1.5875(9)	1.6157(19)	Si1-O4	1.59(1)	Si2-O4	1.603(9)	Si1-O3	1.625(9)	Si2-O7	1.672(9)
Si-O4	1.6145(4)	1.6044(7)	1.6030(15)	Si1-O8	1.603(9)	Si2-O7	1.607(9)	Si1-O1	1.631(7)	Si2-O6	1.696(8)
Si-O1	1.6162(7)	1.617(1)	1.812(2)	Si1-O2	1.621(8)	Si2-O1	1.623(9)	Si1-O2	1.744(9)	Si2-O4	1.724(9)
Si-O2	1.6232(7)	1.5894(8)	1.600(2)	Si1-O6	1.79(1)	Si2-O5	1.787(11)	Si1-O4	1.745(7)	Si2-O8	1.728(9)
		Si-O1*	1.848(2)	Si1-O6	1.81(1)	Si2-O5	1.814(11)	Si1-O4	1.773(9)	Si2-O2	1.837(7)
								Si1-O8	1.861(9)	Si2-O7	1.839(9)
<Si-O>	1.6165	1.5995	1.696		1.6837		1.6872		1.7299		1.7490
Volume	2.165	2.066	4.0737		4.0005		4.0340		6.814		7.024
<i>BO₄</i> tetrahedra											
	<i>BO₄</i>		<i>B1O₄</i>	<i>B2O₄</i>		<i>B1O₄</i>	<i>B2O₄</i>		<i>B2O₄</i>		
B-O5	1.450(1)	1.446(1)	1.456(3)	B1-O7	1.44(1)	B1-O8	1.42(2)	B1-O3	1.398(16)	B2-O2	1.426(15)
B-O3	1.462(1)	1.473(2)	1.471(4)	B1-O1	1.44(2)	B1-O2	1.46(2)	B1-O5	1.445(16)	B2-O5	1.456(13)
B-O1	1.480(1)	1.429(1)	1.461(3)	B1-O5	1.45(2)	B1-O6	1.46(2)	B1-O8	1.476(14)	B2-O6	1.468(17)
B-O2	1.499(1)	1.457(2)	1.444(3)	B1-O3	1.46 (2)	B1-O3	1.46(2)	B1-O7	1.577(13)	B2-O1	1.509(12)
<B-O>	1.473	1.451	1.458		1.4462		1.4504		1.4742		1.464
Volume	1.629	1.556	1.572		1.5313		1.5432		1.6396		1.6063

<i>CaO_n polyhedra</i>											
	<i>CaO₇</i>	<i>CaO₁₁</i>	<i>CaO₁₁</i>	<i>CaO₁₁</i>					<i>CaO₁₂</i>		
Ca-O5	2.3847(11)	2.3218(15)	2.354(3)	Ca-O3	2.309(11)	Ca-O3	2.468(9)	Ca-O6	2.372(8)	Ca-O2	2.515(8)
Ca-O2 (x2)	2.4396(7)	2.3614(8)	2.3614(19)	Ca-O8	2.329(8)	Ca-O6	2.601(9)	Ca-O5	2.404(7)	Ca-O7	2.530(8)
Ca-O3 (x2)	2.4575(7)	2.5392(9)	2.403(2)	Ca-O7	2.339(9)	Ca-O2	2.605(8)	Ca-O8	2.431(8)	Ca-O4	2.566(8)
Ca-O1 (x2)	2.4815(7)	2.4574(8)	2.603(2)	Ca-O1	2.355(9)	Ca-O5	2.615(9)	Ca-O6	2.447(8)	Ca-O1	2.585(9)
Ca-O2* (x2) ^	3.0173(7)	3.2423(9)	3.407(3)	Ca-O2	2.358(11)	Ca-O1	2.613(9)	Ca-O1	2.467(7)	Ca-O3	2.594(8)
Ca-O4*	3.6127(7)	2.6152(12)	2.405(3)	Ca-O4	2.375(9)			Ca-O3	2.504(8)	Ca-O5	2.621(9)
Ca-O5*	3.4788(7)	2.6336(12)	2.516(3)								
Ca-O3*(x2)	4.626	2.8786(11)	2.651(2)								
<Ca-O>	2.4595 /2.5990^	2.549	2.483		2.4511						2.503
Volume	18.774/	36.083	33.791		32.5420						37.030
			28.1962^								

Table S3. Coefficients obtained by fitting the Murnaghan equation of state to the P-V data of danburite up to 23 GPa

Pressure range	V ₀ (Å ³)	K (GPa)	Reference
0 - 7 GPa	545.90(8)	94.1(4)	present study
7 - 23 GPa	602(4)	33(1)	present study
0 - 4.5 GPa	543.8(2)	114(3)	Hackwell & Angel, 1974

* All calculations used K' fixed to 4.0 to provide a consistent basis for comparison between present and previously reported results. The observed difference in K in the low pressure region may indicate that the change in the compression mechanism of danburite has already occurred at 6.5 GPa. The lack of P-V data below 7 GPa (diffraction data was collected at three pressure points) prevented the precise estimation of critical pressure.

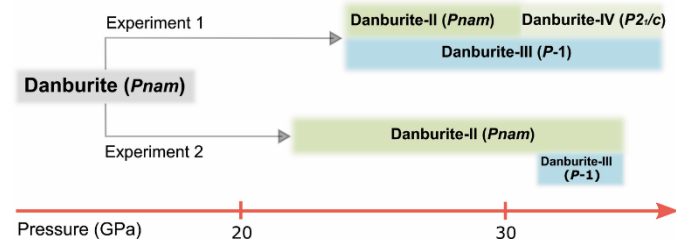


Fig. S1. The transformation routes of danburite in experiments 1 and 2.

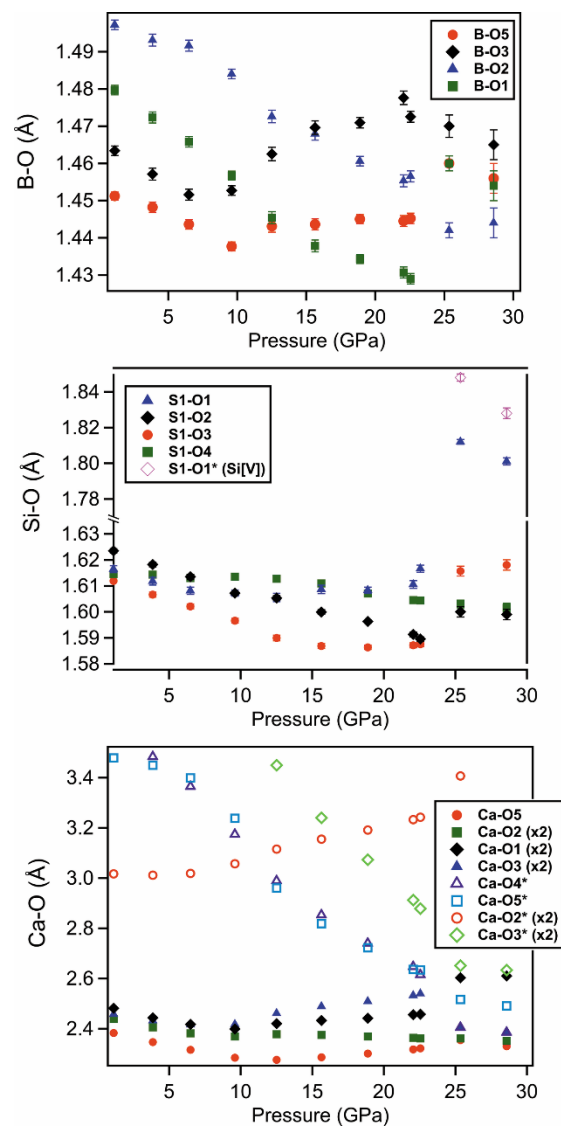


Fig. S2. High-pressure evolution of selected bond distances in *Pnam* phases of danburite.

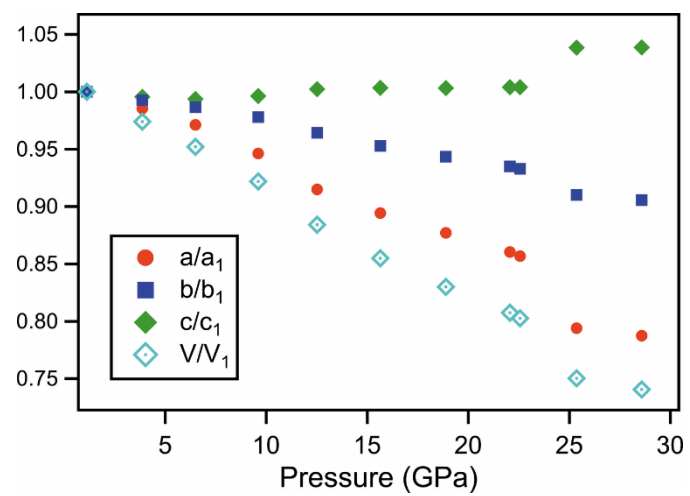


Fig. S3. Evolution of normalized unit-cell parameters of danburite and danburite-II. Data from Experiment 1 are presented.

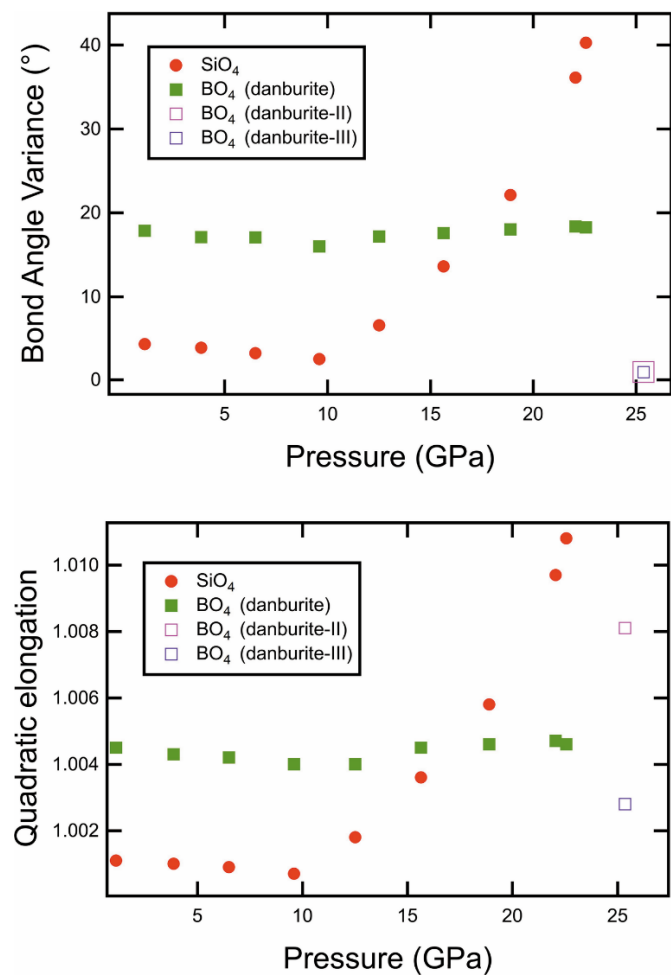


Fig. S4. The evolution of quadratic elongation (QE) and bond angle variance (BAV, °) of SiO_4 and BO_4 tetrahedra along the compression of danburite (Experiment 1). The parameters QE and BAV that show deviation of TO_4 polyhedra from geometry of ideal tetrahedron are defined as: $\text{QE} = \frac{1}{4} \sum_{i=1}^4 \left(\frac{l_i}{l_0} \right)^2$ and $\text{BAV} = \sqrt{\frac{1}{5} \sum_{i=1}^6 (\theta_i - 109.47)^2}$ where l_0 is a centre-to-vertex distance for ideal tetrahedron whose volume is equal to that of the distorted tetrahedron with bond lengths l_i and bond angles θ_i .

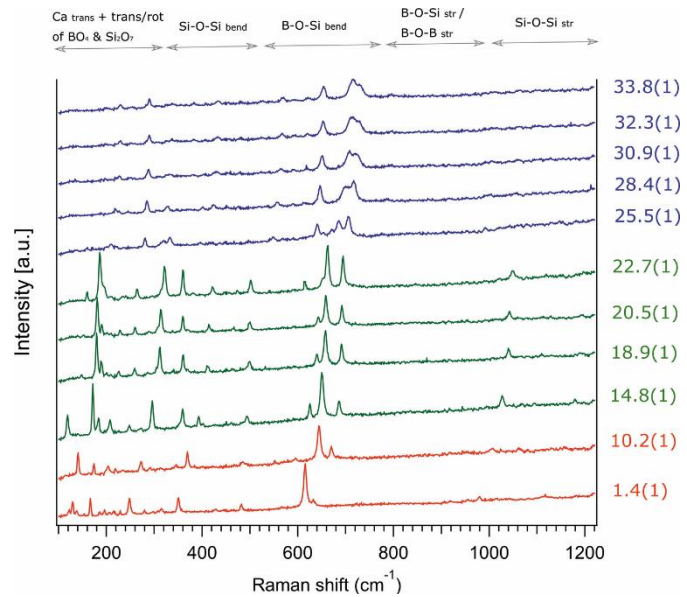


Fig. S5. Evolution of Raman spectra of danburite along the compression. The pressure is given in GPa. The peaks are assigned according to Best et al. (1994) (measurements performed under ambient conditions). Different colours correspond to the high-pressure phases with distinct vibration properties.

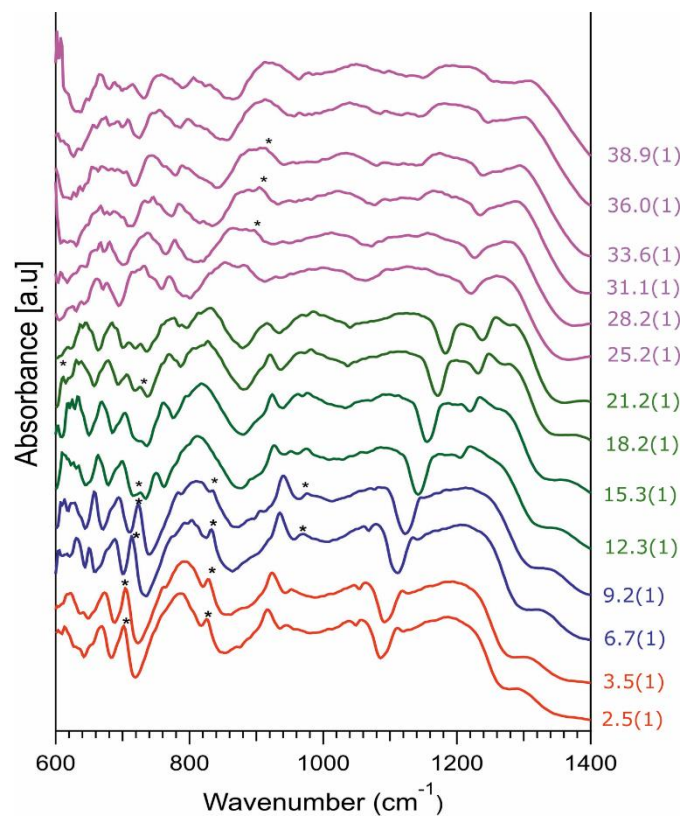


Fig. S6. Evolution of infrared spectra of danburite along the compression. Stars indicate peaks possibly originating from interferences of the beam between the diamond surfaces. The pressure is given in GPa. Different colours correspond to the high-pressure phases with distinct vibration properties.

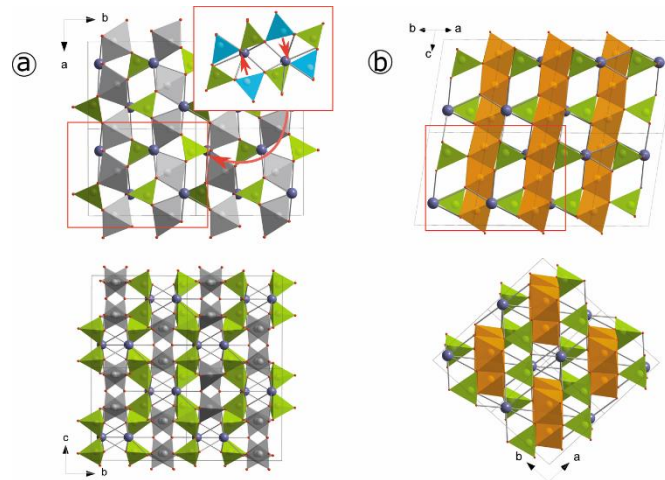


Fig. S7. The crystal structures of high-pressure phases of danburite. (a) The danburite-II ($Pnam$) with five-fold coordinated silicon in trigonal-bipyramidal geometry. The insert shows the mechanism of danburite \rightarrow danburite-II phase transformation, *i.e.* a closure of eight-membered rings at pressures above 22.6(1) GPa. (b) The danburite-III ($P-1$) with octahedrally coordinated silicon. Grey, orange and green polyhedra represent SiO_5 , SiO_6 and BO_4 , respectively.

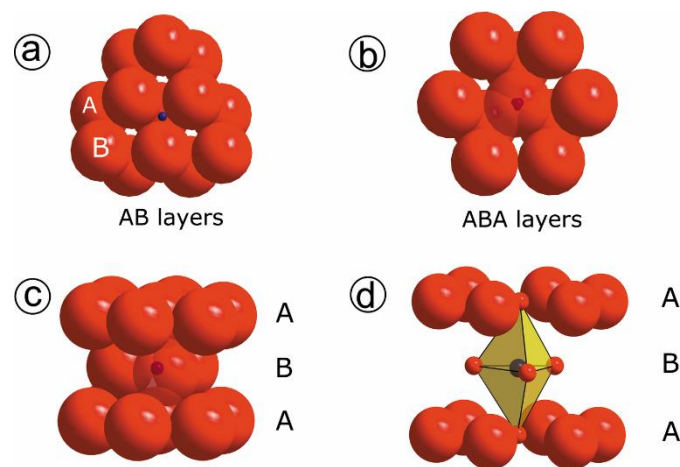


Fig. S8. Pentacoordinated void in a hexagonal close packing with sequence of layers ...ABAB... (a) View of two oxygen layers AB perpendicular to the stacking direction. The blue sphere is located between three oxygens in a layer B and above one oxygen from layer A. (b) A third oxygen layer A is located above layers AB so that now the blue sphere is positioned between five oxygens: three oxygens of layer B and two oxygens from two layers A from below and above. (c) View of the layers ABA along the stacking direction. (d) The coordination polyhedron of the blue sphere possesses geometry of trigonal bipyramidal. For simplicity, size of spheres located in the vertices of trigonal bipyramid is reduced.

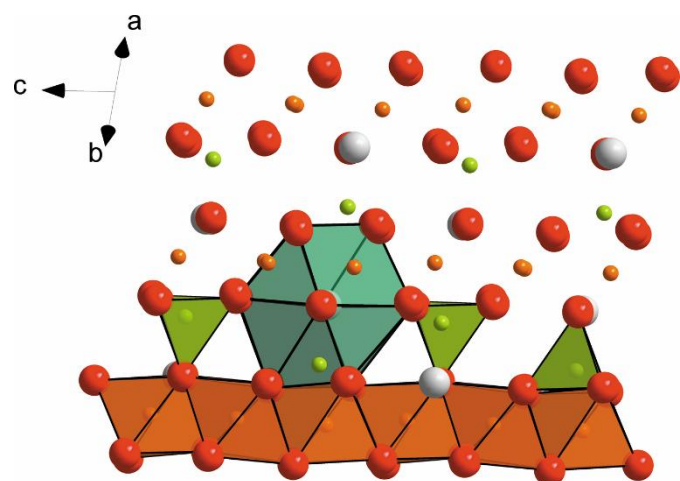


Fig. S9. O and Ca atoms (red and white, respectively) build cubic close packing in the structure of danburite-III (*P*-1). Si atoms (given in orange) occupy octahedral voids while the B atoms (given in green) are placed in tetrahedral voids. CaO₁₂ cubooctahedron is shown in blue.

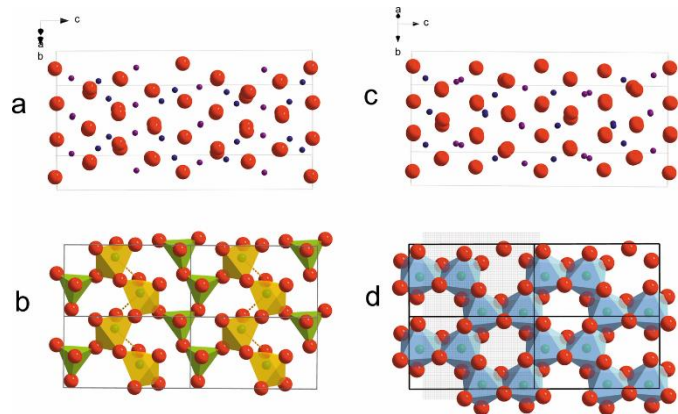


Fig. S10. The evolution of close packing of oxygen atoms in the structure of postorthoenstatite (Finkelstein et al., 2015) and corresponding change in silicon coordination. (a) The ... ABCBACBC... packing of oxygen layers in alpha-postorthoenstatite. (b) The formation of distorted octahedral voids by displacement of oxygen layers. Note the displacement of Si atoms from the centre of the quasi-octahedral voids; the corresponding long non-bond contact is shown as a dashed line. (c) The hexagonal ..AB.. close packing in the structure of beta-postorthoenstatite . (d) The silicon atoms occupy octahedral voids.